ImmunoTargets and Therapy

Dovepress
Taylor & Francis Group

Open Access Full Text Article

ORIGINAL RESEARCH

Clinical Risk Stratification and Modifiable Risk Factors for Hepatitis B Virus-Related Follicular Lymphoma

Yuwei Deng[1], Zhenyuan Jia[1], Huilai Zhang[2], Xiaosan Zhang[3], Lihong Liu[4], Xianhuo Wang[2], Hongtao Song[5], Zirong Zhang[6], Caili Liu[6], Qingyuan Zhang[1], Jianli Ma[7]

[1]Department of Medical Oncology, Harbin Medical University Cancer Hospital, Harbin, Heilongjiang, People's Republic of China; [2]Department of Lymphoma, Tianjin Medical University Cancer Institute and Hospital, Tianjin, People's Republic of China; [3]Department of Medical Oncology, Henan Cancer Hospital, Zhengzhou, Henan, People's Republic of China; [4]Department of Hematology, The Fourth Hospital of Hebei Medical University, Hebei Provincial Key Laboratory of Tumor Microenvironment and Drug Resistance, Shijiazhuang, Hebei, People's Republic of China; [5]Department of Pathology, Harbin Medical University Cancer Hospital, Harbin, Heilongjiang, People's Republic of China; [6]Department of Hematology, The Fourth Hospital of Hebei Medical University, Shijiazhuang, Hebei, People's Republic of China; [7]Department of Radiation Oncology, Harbin Medical University Cancer Hospital, Harbin, Heilongjiang, People's Republic of China

Correspondence: Jianli Ma, Department of Radiation Oncology, Harbin Medical University Cancer Hospital, Harbin, Heilongjiang, People's Republic of China, Tel +86-18686837985, Email 601959@hrbmu.edu.cn; Qingyuan Zhang, Department of Medical Oncology, Harbin Medical University Cancer Hospital, Harbin, Heilongjiang, People's Republic of China, Tel +86-13313612989, Email 0566@hrbmu.edu.cn

Background: Hepatitis B virus (HBV) infection (surface antigen positive, HBsAg+) has been related to the increased risk in follicular lymphoma (FL). The further understanding of features in HBV-associated FL remains lacking.

Methods: We explored clinical risk factors in HBsAg-positive patients from multicentric clinical investigation retrospectively (n = 276) and integrated HBV-related factors into Follicular Lymphoma International Prognostic Index (FLIPI) scoring system for risk prediction. The methylation profiles in pre- and paired HBsAg+FL occurring progression of disease within 2 years (POD24) were determined using the Human Methylation 850K BeadChip platform. Bulk RNA sequencing was performed for gene expression in samples from the same patient and confirmed using $Myc^{Cd19Cre}$ C57BL/6J chimera mice.

Results: We found that HBsAg+ FL with a higher incidence of POD24. The high HBV-DNA load (>10^5 copies/mL) was identified as a pivotal risk factor. HBsAg+ FL with the rapidly decreasing viral load showed lower incidence of POD24 than those without viral control (P = 0.026). Integrated risk stratification incorporating HBV-related clinical parameters based on FLIPI scoring systems had potential predictive value for high-risk patients (AUC = 0.616, P = 0.002). The methylation profiles in pre-POD24-HBsAg+FL and paired POD24-HBsAg+FL showed distinguished signatures of methylated *KMT2A*, *EP300-AS1*, *ARID1B*, *MHC I* class molecular genes related to tumor cells, and *TNFRSF1A*, *LTA*, *IQCE* genes related to immune cells. Of note, we confirmed that the crucial CXCR5 mRNA expression with specific methylated regions was inversely correlated to featured MYC mRNA expression as "trans" regulation in both POD24-HBsAg+FL and $Myc^{Cd19Cre}$ lymphoma model.

Conclusion: Integrated clinicopathological features into prediction system may provide precise risk stratification for HBV-positive FL. Modifiable DNA methylation acts as the potential targets for the combined treatment strategy to delay POD24 occurrence.

Plain Language Summary: Based on the retrospective clinical data from multiple clinical centers of China, we first present the clinical characteristics associated with chronic hepatitis B virus (HBV) infection and illustrated their prognostic roles in follicular lymphoma. We novelly integrated HBV-related risk factors into the canonical Follicular Lymphoma International Prognostic Index scoring. We revealed that modifiable genes methylation,especially in genes which regulated immune response, was associated with the early relapse of disease. The myelocytomatosis oncogene (MYC) is the driver for the aggressive progression of B-cell lymphoma in multiple clinical guidelines. Of note, we further confirmed that Chemokine C-X-C-Motif Receptor 5 (CXCR5) mRNA expression with specific methylated regions was inversely correlated to MYC mRNA expression during the disease progression, showing the potential promotion of immune activities on tumor progression. Our study provided the potential targets to delay the disease progression within 24 months (POD24) through reversing methylation modification in the further epigenetic molecular treatment.

Keywords: follicular lymphoma, hepatitis B virus, POD24, risk prediction, methylation, MYC, CXCR5

Received: 3 June 2025
Accepted: 6 November 2025
Published: 12 November 2025

Graphical Abstract

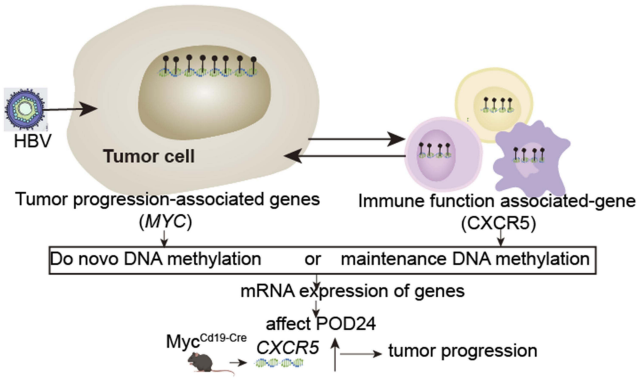

Introduction

Follicular lymphoma (FL) is the most frequent indolent lymphoma, showing discordant incidence of all newly diagnosed non-Hodgkin lymphomas (NHLs) in the Western countries with 20–25%[1] and in China with 10–12%.[2] The experienced strategy of watchful waiting is for asymptomatic patients with advanced-stage and low-tumor-burden,[3] and CD20-directed immunochemotherapy is served as standard first-line therapy of advanced-stage FL.[4] Numerous evidences have revealed the 2–3-fold high risk of chronic hepatitis B virus (HBV) surface antigen (HBsAg)-positive infections to develop B-cell NHLs including FL, which exhibits poor overall survival (OS) and a high incidence of disease progression within 24 months (POD24).[5] China is featured with a high prevalence of the HBV infection. HBV confers chemoresistance,[6] and the selection of time to start the treatment and the proper therapeutic regimens including immunochemotherapy and anti-viral prophylaxis remains the great challenges to improve survival.[7,8]

There are multiple clinical prognostic models to stratify the risk categories in FL patients with useful practices, including the classical Follicular Lymphoma International Prognostic Index (FLIPI) and FLIPI-2.[9,10] But they are not accurate enough to guide treatment strategies.[4] Recently, the clinicogenomic models such as m7-FLIPI scoring with seven genes, a developed 23-gene signature model which captures various aspects in tumor biology, and BioFLIPI which integrates the microenvironment biomarker, could bring to precision medicine.[11] However, due to the markedly distinct outcomes in HBV-related FL differing from general FL populations,[5,12] these models ignored key factors derived from virus infection such as virus loads.[13] Clinically, although some HBV-infected patients with low or intermediate FLIPI scoring, they also suffered early progression.

Studies have disclosed distinct genetic/epigenetic features in FLs. For example, EZH2 as histone methyltransferase (H3K27me3) plays crucial role in differentiation and function of germinal center B cells (GCB) and immune remolding. The *EZH2* inhibitor (eg tazemetostat) has acquired US food and Drug Administration (FDA) approval for relapsed / refractory (R/R) FL.[14] Other epigenetic modifiers, such as *BCL7A*, ARID1A/B and KMT2D, all commonly shared in multiple disease stages (initial, progression, transformation) and were potentially insufficient to be well compared.[15] It is worth noting that HBV infection has various impacts on the natural immune response.[16] Considering the influence from viral infection on immune regulations, the more aspects of epigenetic modification in lymphoma B cells beyond EZH2-dependent mechanism remains uncertain.

This study aimed to explore the risk factors derived from the HBV infection for integrative prognostic stratification based on FLIPI scoring in FL. The distinct methylation signatures of immune-regulation genes between pre-POD24-HBsAg+FL and paired POD24-HBsAg+FL were explored for better auxiliary understanding of the impact from HBV infections and provided the novel choice of epigenetic treatment strategies in future.

Materials and Methods

Patients

Totally 276 patients were retrospectively reviewed and confirmed the diagnosis of follicular lymphoma by an experienced haematopathologist between January 2010 and January 2022 from Harbin Medical University Cancer Hospital (n = 104), the Tianjin Medical University Cancer Institute and Hospital (n = 73) and the Fourth Hospital of Hebei Medical University (n = 99). All patients had previously given informed consent. Patients who were asymptomatic and the low tumor burden retained watchful waiting as the initial strategy until disease progression. The advanced-stage patients underwent rituximab-containing immunochemotherapy. Patients with a high tumor burden and responding well to initial treatment would receive rituximab-maintenance therapy. Patients with high HBV DNA load (>10^4 copies/mL)[17] received chemotherapy without rituximab. All the HBsAg+ patients were given antiviral prophylaxis. POD24 referred to progression or relapse of the disease within the initial 24 months after diagnosis following the first-line therapy. The FLIPI score was calculated based on international criterion as previous.[4] All experiments involving human patients were approved by the Research Ethics Committee of Harbin Medical University Cancer Hospital (Approval no. KY2023-79) in accordance with the Declaration of Helsinki. Personal data were anonymized in the study. The cohort study was conducted complying with the STROBE guideline.

Construction and Validation of Risk Stratification

Risk score was calculated for each patient as a weighted sum of HBV infection-related factors determined by the univariable and multivariable Cox proportional hazard regression and FLIPI scoring using linear regression (eigenvalue, Supplementary Table 1). The integrative score for each patient was calculated as total sum of each epigenvalue for positive factors. We estimated the optimal cutoff value to maximize the Wald statistic by the Receiver Operating Characteristic (ROC) curve and dichotomized patients into high-risk and low-risk subgroups. Kaplan-Meier Log rank test was used to estimate the prognosis. Patients who were alive or experienced PD were censored at the last date known alive or at their last disease assessment. Patients were not evaluable for POD24 if they were censored (eg, lost to follow-up) or died within 24 months without progression of disease. The internal validation (n = 35) from Harbin Medical University Cancer Hospital and the external validation (n = 153) from the Shandong University Cancer Center, the First Affiliated Hospital of Harbin Medical University, and the Henan Cancer Hospital, were performed after acquiring informed consents and receiving the approval by the Research Ethics Committee of these centers. The same inclusion and exclusion criteria of these cohorts as abovementioned aligned with study cohorts.

Illumina DNAm EPIC Analysis

DNA Methylation Experiment

The Formalin Fixed Paraffin Embedded samples of paired pre- and post-lymph node biopsies from HBsAg+ patients with POD24 after cyclophosphamide, doxorubicin, vincristine and prednosine plus rituximab (R-CHOP) or bendamustine plus rituximab (BR) treatment (excluding the histological transformation) were obtained. The DNA was separated by application of the DNeasy Blood and Tissue Kit (Qiagen). The Nanodrop 2000 (Thermo) was used to assess the purity and concentration of DNA. EZ DNA Methylation Kits (Zymo Research, USA) and the 850K BeadChips with 820,000 probes were applied to detect the converted products as per the manufacturer's instruction (Illumina).

Data Analysis

The data were primarily analyzed by a ChAMP package in R with the normalized β-value matrix. The EPICanno.ilm10b4.hg19 was used to annotate all CpG sites. Differential Methylated CpGs Positions (probes) were calculated through the champ with adjusted p values by the Benjamini–Hochberg method. CpGs with $|\Delta\beta| \geq 0.20$ and DMPs with adjusted $p \leq 0.05$ were defined. Functional Epigenetic Modules reflect protein to protein interaction network (PPI) using the FEM package. A Conumee package was applied to analyze the copy number variation. The proportions of the immunocytes were estimated by the EpiDISH16 and HEpiDISH17 methods as indicated previously.[18] The two-factor ANOVA was conducted for statistical analysis with the *P*-value and *F*-value.

Myc-Driven B-Cell Lymphoma Chimeric Mice Model

The experimental procedures of mice were performed in stringent accordance with the institutional guidelines delineated by Harbin Medical University, as per the Guide for the Care and Use of Laboratory Animals and standards established by the Association for Assessment and Accreditation of Laboratory Animal Care International. The Southern Model Biology Research Center (Shanghai) and the Institutional Animal Care and Use Committee of Harbin Medical University, having vetted all procedures, duly approved the entirety of the study involving mice under protocols #HMUIRB2025004, and #SCXK (shanghai) 2019-0002. The experimental mice were age- and sex-matched, ranging from 8 to 10 weeks. No evidence of sex-based influences or biases was observed. The following strains were obtained from The Southern Model Biology Research Center (Shanghai): H11-CAG-LSL-Myc (strain NM-KI-00039), Cd19-Cre (NMX) (strain NMX-KI -190023). Using CRISPR/Cas9 technology, heterozygous mice with targeted conditional overexpression of Myc in the H11 gene were obtained. The CD19-Cre knock-in/knock-out allele has a Cre recombinase gene inserted into the first coding exon of the CD19 antigen gene as protocol (JAX stock #006785). They were back-crossed to C57BL/6J genetic background through at least six generations before used for experiments.

NP (4-hydroxy-3-nitrophenyl acetyl) was conjugated to CGG (Chicken γ-globulin) at a ratio of NP18-CGG (BiosearchTM technologies, IMMB1-003). Myc-Cd19-Cre or wild-type mice were immunized intraperitoneally with 100ug alum (Biodragon, KX0210054) precipitated 50 μg NP18-CGG. Superficial lymph nodes were analyzed. All the animal studies designs were performed complying with the ARRIVE guidelines.

Bulk RNA Sequencing

RNA was extracted from patients with POD24 or mice lymph node tissues by column purification using FFPE RNA extraction kit (Meji, IVD4144) and total RNA extraction kit (Tiangen, DP419). The RNA samples were strictly quality controlled reaching at least 100ng. Library construction was performed according to the Hieff NGS MaxUp Human rRNA Depletion Kit (rRNA and ITS/ETS) item number 12257ES96 or Poly (A) (Hieff NGS mRNA Isolation) Master Kit V2, No. 12629ES96). The purified double-stranded cDNA was subjected to end repair, A-tail addition, sequencing adapter, PCR amplification, and DNA purification beads to purify the PCR products. The library connector used a MGI connector with a double-ended index tag. The different libraries were pooled according to the requirements of effective concentration and target amount of data, and then DNBSEQ-T7 PE100 sequencing was performed. PE100 (Pair End 100 bp) refers to high-throughput double-end sequencing, with 100 bp at each end. Combined analysis was performed based on 935K data and Gene expression data of RNA chip of pre-POD24-HBsAg+FL and paired POD24-HBsAg+FL samples.

Statistical Analysis

Statistical analyses were performed by SPSS 25.0 version software (SPSS Inc. Chicago, USA), R version 4.1.3 or GraphPad Prism 9 with p value. The χ^2-test was performed for categorical variables. Univariable and multivariable Cox proportional hazards regression was applied for the comparisons of PFS and OS by factor categories. Survival data using Kaplan–Meier curves were assessed differences between groups through the Log rank test. Groups were compared using an unpaired t test, Mann Witney U-test or ANOVA with Tukey's post hoc test depending on the number of groups and distribution. The p value was <0.05 for significance (two-sided).

Results

Clinicopathological Features

Of the total 276 patients, 131 patients were seropositive for HBsAg at baseline across the analysis population (FL, n = 276). Shown by serum HBsAg arm, 42 (32.1%) patients with HBsAg+ had a high HBV DNA load ($>10^5$ copies/mL). HBsAg+ patients had more nodal sites with larger sizes (32.8% vs 17.9%, $P = 0.004$) and higher incidence of POD24 (31.3% vs 22.1%, $P = 0.031$) than HBsAg− patients. There was no difference in the incidence of an absolute lymphocyte count (ALC) <1000/μL ($P = 0.630$) between the two arms (Table 1).

Table 1 Patient Characteristics Summary in Study and External Validation Groups

	Study Group (n = 276)			External Validation Group (n=153)		
	HBsAg+ FL (%)	**HBsAg− FL (%)**	***P* values**	**HBsAg+ FL (%)**	**HBsAg− FL (%)**	***P* values**
No. of patients	131	145		24	129	
Age (years)[a]						
≤60	49 (37.4)	62 (42.8)	0.365	5 (20.8)	24 (18.6)	0.798
>60	82 (62.6)	83 (57.2)		19 (79.2)	105 (81.4)	
Sex						
Female	64 (48.9)	80 (55.2)	0.294	11 (45.8)	60 (46.5)	0.491
Male	67 (51.1)	65 (44.8)		13 (54.2)	69 (53.5)	
Ann Arbor stage						
I–II	26 (19.8)	25 (17.2)	0.578	2 (8.3)	21 (16.3)	0.317
III–IV	105 (80.2)	120 (82.8)		22 (91.7)	108 (83.7)	
Grade						
1–2	70 (53.4)	95 (65.5)	0.210	15 (62.5)	80 (62.0)	0.415
3A	46 (35.1)	41 (28.3)		5 (20.8)	38 (29.5)	
3B	8 (6.1)	3 (2.1)		3 (12.5)	10 (7.8)	
3 (mix 3A and 3B)	4 (3.1)	4 (2.8)		1 (4.2)	1 (0.8)	
3A/B mixed DLBCL	3 (2.3)	2 (1.4)		0 (0)	0 (0)	
B symptoms						
Present	23 (17.6)	30 (20.7)	0.509	4 (16.7)	6 (4.7)	**0.029**
Absent	108 (82.4)	115 (79.3)		20 (83.3)	123 (95.3)	
ECOG PS						
0, 1	126 (96.2)	140 (96.6)	0.870	18 (75.0)	102 (79.1)	0.102
≥2	5 (3.8)	5 (3.4)		6 (25.0)	27 (20.9)	
Number of nodal sites ≥5						
Present	55 (42.0)	65 (44.8)	0.634	7 (29.2)	35 (27.1)	0.837
Absent	76 (58.0)	80 (55.2)		17 (70.8)	94 (72.9)	
BM involvement						
Present	18 (13.7)	38 (26.2)	**0.010**	8 (33.3)	50 (38.8)	0.053
Absent	113 (86.3)	107 (73.8)		16 (66.7)	79 (61.2)	
Extranodal involvement[b]						
Present	63 (48.1)	70 (48.3)	0.547	8 (33.3)	28 (21.7)	0.218
Absent	68 (51.9)	75 (48.3)		16 (66.7)	101 (78.3)	

(*Continued*)

https://doi.org/10.2147/ITT.S543117

Table 1 (Continued).

	Study Group (n = 276)			External Validation Group (n=153)		
	HBsAg+ FL (%)	**HBsAg− FL (%)**	***P* values**	**HBsAg+ FL (%)**	**HBsAg− FL (%)**	***P* values**
Tumor with a diameter ≥7 cm						
Present	23 (17.6)	15 (10.3)	0.082	2 (8.3)	10 (7.8)	0.923
Absent	108 (82.4)	130 (89.7)		22 (91.7)	119 (92.2)	
≥3 nodal sites, each ≥3 in diameter						
Present	43 (32.8)	26 (17.9)	**0.004**	9 (37.5)	11 (8.5)	**0.015**
Absent	88 (67.2)	119 (82.1)		15 (62.5)	118 (91.5)	
Hemoglobin level						
<12 g/dL	28 (21.4)	24 (16.6)	0.306	3 (12.5)	16 (12.4)	0.989
≥12 g/dL	103 (78.6)	121 (83.4)		21 (87.5)	113 (87.6)	
LDH						
Elevated	30 (22.9)	35 (24.1)	0.809	5 (20.8)	28 (21.7)	0.924
Normal	101 (77.1)	110 (75.9)		19 (79.2)	101 (78.3)	
Albumin						
<3.5 g/dL	13 (10.0)	8 (5.5)	0.162	3 (12.5)	9 (7.0)	0.206
≥3.5 g/dL	118 (90.0)	137 (94.5)		21 (87.5)	120 (93.0)	
ALC						
<1000 /μL	4 (3.1)	6 (4.1)	0.630	3 (12.5)	13 (10.1)	0.328
≥1000 /μL	127 (96.9)	139 (95.9)		21 (87.5)	116 (89.9)	
HBV DNA load						
Low (<10^5 copies/mL) or absent	89 (67.9)	145 (100.0)	**<0.001**	16 (66.7)	129 (100.0)	**<0.001**
High (>10^5 copies/mL)	42 (32.1)	0 (0)		8 (33.3)	0 (0)	
Hepatitis B e antigen						
Positive	19 (14.5)	6 (4.2)	**<0.001**	5 (20.8)	11 (8.5)	**<0.001**
Negative	112 (85.5)	139 (95.8)		19 (79.2)	118 (91.5)	
FLIPI risk groups						
Low	13 (9.9)	51 (35.2)	**<0.001**	9 (37.5)	41 (31.8)	**0.041**
Intermediate	43 (32.8)	61 (42.1)		8 (33.3)	58 (45.0)	
High	75 (57.3)	33 (22.8)		7 (29.2)	30 (23.3)	
Initial treatment strategy						
R-CHOP like	77 (58.8)	83 (57.2)	**<0.001**	14 (58.3)	78 (60.5)	**<0.001**
CHOP	42 (32.1)	10 (6.9)		8 (33.3)	6 (4.7)	
BR	10 (7.6)	47 (32.4)		2 (8.3)	26 (20.2)	
Others[c]	2 (1.5)	5 (3.4)		0 (0)	19 (14.7)	

(*Continued*)

Table 1 (Continued).

	Study Group (n = 276)			External Validation Group (n=153)		
	HBsAg+ FL (%)	**HBsAg− FL (%)**	***P* values**	**HBsAg+ FL (%)**	**HBsAg− FL (%)**	***P* values**
Rituximab maintenance						
Present	31 (23.7)	28 (19.3)	0.378	4 (16.7)	42 (32.6)	0.119
Absent	100 (76.3)	117 (80.7)		20 (83.3)	87 (67.4)	
POD24						
Present	41 (31.3)	32 (22.1)	**0.031**	9 (37.5)	38 (29.5)	**0.033**
Absent[d]	90 (68.7)	113 (77.9)		15 (62.5)	91 (70.5)	
Histological transformation (DLBCL)						
Present	13 (9.9)	13 (9.0)	0.786	1 (4.2)	6 (4.7)	0.917
Absent	118 (90.1)	132 (91.0)		23 (95.8)	123 (95.3)	
Combined hepatitis[c]						
Present	3 (2.3)	1 (0.7)	0.267	1 (4.2)	4 (3.1)	0.787
Absent	128 (97.7)	144 (99.3)		23 (95.8)	125 (96.9)	
Viral load decline within 1 month						
Yes	70 (53.4)	0 (0)	**<0.001**	19 (79.2)	0 (0)	**<0.001**
No	61 (46.6)	0 (0)		5 (20.8)	0 (0)	
Absent	0 (0)	145 (100.0)		0 (0)	129 (100.0)	
Watchful waiting						
Yes	13 (9.9)	18 (12.4)	0.513	3 (12.5)	20 (15.5)	0.705
No	118 (90.1)	127 (87.6)		21 (87.5)	109 (84.5)	

Notes: [a]Median (range). [b]Extranodal sites of involvement other than BM. [c]R-FC fludarabine and cyclophosphamide plus rituximab; R2 lenalidomide plus rituximab. [d]Absence of POD24 included those who had no occurrence of event and who were not available for the evaluation (death within 24 months and watch-for waiting). *P* value <0.05 was showed in bold.

Abbreviations: HBsAg, hepatitis B surface antigen; ECOGPS, Eastern Cooperative Oncology Group Performance Status; BM, bone marrow; LDH, lactate dehydrogenase; ALC, absolute lymphocyte count; FLIPI, Follicular Lymphoma International Prognostic Index; CHOP, cyclophosphamide, doxorubicin, vincristine and prednisone plus rituximab; R-CHOP, cyclophosphamide, doxorubicin, vincristine and prednosine plus rituximab; BR, bendamustine plus rituximab; CT, chemotherapy; DLBCL, diffuse large B cell lymphoma; CR, complete remission; PR, partial remission; SD, stable disease; PD, progressive disease; POD24, progression of disease within 24 months.

Totally 131 patients with HBsAg+ were summarized in Table 2. The older age (>60 years, 35.4% vs 24.5%, P = 0.034), high HBV DNA at baseline (52.4% vs 21.3%, $P < 0.01$), HBeAg-positive at baseline (42.1% vs 28.2%, P = 0.022), and low ALC at baseline (50.0% vs 30.7%, P = 0.045), demonstrated a higher incidence of POD24 events. But rapidly decreasing HBV DNA (<10^3 IU/mL) within 1 month after prophylactic nucleoside analogues treatment (NAT) exhibited a lower incidence of POD24 (22.9% vs 41.0%, P = 0.026). The FLIPI scoring was not significantly associated with the incidence of POD24 (P = 0.226) (Table 2). Seventy-three patients occurred POD24 and those with HBsAg+ had a higher rate of histological transformation than HBsAg− patients (7.3% vs 3.1%, P = 0.046) (Supplementary Table 2).

Risk Analysis of HBV Infection on Prognosis

An overall median follow-up in HBsAg+ patients was 38.7 months (IQR, 28.9–51.5).

Patients with HBsAg+ showed a shorter progression-free survival (PFS, log-rank P = 0.004, Figure 1A) and OS (P = 0.039, Figure 1B) than those with HBsAg−. In non-POD24 arm, HBsAg+ patients also had shorter PFS (P = 0.036, Figure 1C) and OS (P = 0.007, Figure 1D) compared with HBsAg− patients. In cases of POD24, HBsAg+ indicated no

https://doi.org/10.2147/ITT.S543117

Table 2 Correlation Analysis Between the POD24 Event and Clinical Parameters in HBsAg+ FL Subgroup

	POD24 N (%)		*P* values
	Present	**Absent**	
Age (years)			
≤60	12 (24.5)	37 (75.5)	**0.034**
>60	29 (35.4)	53 (64.6)	
Viral load decline within 1 month			
Yes	16 (22.9)	54 (77.1)	**0.026**
No	25 (41.0)	36 (59.0)	
HBV DNA load			
Low (<10^5 copies/mL)	19 (21.3)	70 (78.7)	**<0.001**
High (>10^5 copies/mL)	22 (52.4)	20 (47.6)	
Hepatitis B e antigen			
Present	8 (42.1)	11 (57.9)	**0.022**
Absent	31 (28.2)	79 (71.8)	
ALC			
<1000 /μL	2 (50.0)	2 (50.0)	**0.045**
≥1000 /μL	39 (30.7)	88 (69.3)	
FLIPI			
Low	3 (23.1)	10 (76.9)	0.226
Intermediate	10 (23.3)	33 (76.7)	
High	28 (37.3)	47 (62.7)	

Note: P value <0.05 was showed in bold.
Abbreviations: HBsAg, hepatitis B surface antigen; ALC, absolute lymphocyte count; FLIPI, Follicular Lymphoma International Prognostic Index.

obvious correlation with OS (P = 0.896, Figure 1E). The similar association between HBsAg+ and POD24 risk was observed in an external validation cohort (Table 1 and Supplementary Figure 1). There was an association between shorter survival and high HBV-DNA load, but not HBeAg status (Supplementary Figure 2). The HBsAg+ was not an independent prognostic factor for PFS and OS (Tables 3 and 4). Among the HBsAg+ arm, decreased ALC, high HBV-DNA load, persistent viral load after prophylactic NAT, and treatment with BR regimen were associated with shorter PFS (Table 5).

HBV-Related Factors Combined with FLIPI Improves Risk Stratification

Cox proportional regression analysis identified five risk factors for prognostic stratification involving in HBsAg, viral load decline after NAT, HBV DNA load, ALC and treatment strategies. We calculated another risk model using linear regression analysis in which HBV DNA load had the highest scores with eigenvalue of 1.029 (Supplementary Table 1), which could specially predict POD24 in HBV-associated FL patients with cutoff values as 3.236 for risk stratification by dichotomy (Area Under Curve (AUC) = 0.616, P = 0.002) (Figure 2A). Notably, in the study cohort, the model had a higher sensitivity to predict POD24 compared to the FLIPI score (35.8% versus 29.6%) (Figure 2B). The high-risk model was associated with significantly shorter OS (median OS of 67.7, P < 0.01), outperformed that in high-risk FLIPI (OS of 69.8; P < 0.01, Figure 2C). The internal validation cohort and external validation cohort confirmed that the model also had a higher sensitivity for POD24 prediction than FLIPI scoring (40.0% versus 33.3%; 39.1% versus 29.7%, respectively, Figure 2B). Meanwhile, the high-risk model in internal validation cohort (Figure 2D) and external validation cohort (Figure 2E) was related to shorter OS (62.1, P = 0.009; 58.8, P < 0.01, respectively), outperformed that in high-risk FLIPI (70.5, P = 0.038; 69.4, P < 0.01, respectively), albeit at the cost of lower specificity (Figure 2A).

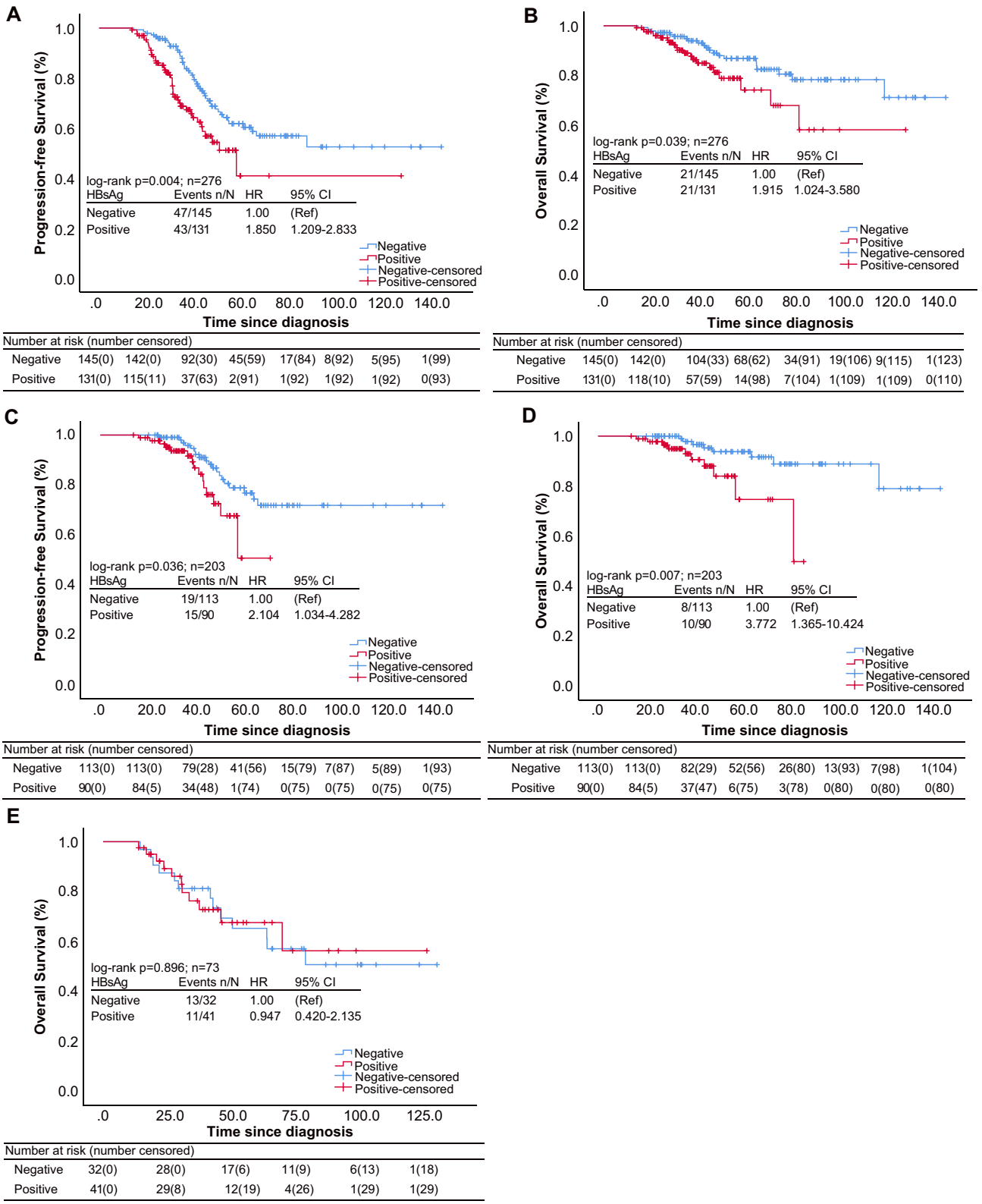

Figure 1 Kaplan–Meier survival curves in study cohort (n = 276), stratified by the presence of hepatitis B surface antigen (HBsAg) at diagnosis. Patients in the HBsAg+ group had worse (**A**) progression-free survival (PFS) and (**B**) overall survival (OS) compared with those in the HBsAg− group. In non-POD24 subgroup, patients in the HBsAg+ group had poorer PFS (**C**) and OS (**D**) compared with the HBsAg− group. In POD24 subgroup, there was no significant difference of OS (**E**) between HBsAg+ group and HBsAg− group.

https://doi.org/10.2147/ITT.S543117

Table 3 Univariable and Multivariable Cox Regression Analysis with Respect to Progression-Free Survival of Clinicopathological Variables

	Univariate Analysis			Multivariate Analysis		
	HR	**95% CI**	**P value**	**HR**	**95% CI**	**P value**
Age (>60 vs ≤60)	1.457	0.963–2.205	0.073*	1.608	1.037–2.493	0.034
Sex (male vs female)	0.876	0.578–1.325	0.529			
Grade (3A vs 1–2)	1.335	0.860–2.073	0.196			
Ann Arbor stage (III/IV vs I/II)	1.174	0.725–1.900	0.513			
Number of extranodal sites (<5 vs ≥5)[a]	0.737	0.486–1.118	0.150			
B symptoms (yes vs no)	1.679	1.028–2.741	0.036*	2.023	1.142–3.584	0.016
BM involvement (no vs yes)	0.666	0.370–1.199	0.173			
High FLIPI risk	3.081	1.740–5.454	<0.001*	1.972	1.023–3.803	0.043
Elevated LDH level	1.317	0.829–2.092	0.242			
Serum albumin <3.5 g/dL	2.633	1.315–5.270	0.004*	1.465	0.649–3.309	0.358
ALC <1000 /μL	1.581	0.641–3.898	0.316			
HBsAg positivity	1.850	1.209–2.833	0.004*	1.184	0.705–1.991	0.523
HBeAg positivity	1.668	0.768–3.623	0.192			
High HBV-DNA load (>10^5 copies/mL)	4.110	2.360–7.160	<0.001*	3.774	1.958–7.278	<0.001
Treatment (BR vs R-CHOP)	1.261	0.752–2.113	0.379			

Notes: *All potential prognostic factors for progression-free survival with a *P* value less than 0.1 in the univariate analysis were selected for multivariate analysis using the backward elimination method (Wald test). [a]Extranodal sites of involvement other than BM.

Abbreviations: FL, follicular lymphoma; HR, hazard ratio; CI, confidence interval; FLIPI, Follicular Lymphoma International Prognostic Index; ECOGPS, Eastern Cooperative Oncology Group Performance Status; BM, bone marrow; ALC, absolute lymphocyte count; HBsAg, hepatitis B surface antigen; HBeAg, hepatitis B e antigen; R-CHOP, cyclophosphamide, doxorubicin, vincristine and prednosine plus rituximab; BR, bendamustine plus rituximab.

Table 4 Univariable and Multivariable Cox Regression Analysis with Respect to Overall Survival in All Baseline Parameters

	Univariate Analysis			Multivariate Analysis		
	HR	**95% CI**	***P* value**	**HR**	**95% CI**	***P* value**
Age (>60 vs ≤60)	2.346	1.246–4.418	0.007*	2.629	1.306–5.291	0.007
Sex (male vs female)	0.758	0.413–1.389	0.368			
Grade (3A vs 1–2)	2.258	1.158–4.045	0.018*	1.238	0.907–1.690	0.179
Ann Arbor stage (III/IV vs I/II)	1.009	0.495–2.060	0.979			
Number of extranodal sites (<5 vs ≥5)[a]	0.712	0.383–1.324	0.281			
B symptoms (yes vs no)	2.663	1.398–5.074	0.002*	3.172	1.449–6.945	0.004
BM involvement (no vs yes)	0.730	0.307–1.734	0.474			
High FLIPI risk	3.757	1.313–10.752	<0.001*	3.638	1.206–10.971	0.022
Elevated LDH level	2.045	1.087–3.850	0.024*	1.146	0.491–2.670	0.753
Serum albumin <3.5 g/dL	5.080	2.215–11.650	<0.001*	1.950	0.630–6.036	0.247
ALC <1000 /μL	0.518	0.071–3.766	0.508			
HBsAg positivity	1.915	1.024–3.580	0.039*	1.179	0.558–2.490	0.667
HBeAg positivity	1.342	0.411–4.375	0.625			
HBV-DNA load (>10^5 copies/mL)	2.851	1.291–6.298	0.007*	1.358	0.518–3.560	0.533
POD24	3.806	2.064–7.019	<0.001*	3.389	1.771–6.487	<0.001*
Treatment (BR vs R-CHOP)	1.639	0.808–3.325	0.171			

Notes: *All potential prognostic factors for progression-free survival with a *P* value less than 0.1 in the univariate analysis were selected for multivariate analysis using the backward elimination method (Wald test). [a]Extranodal sites of involvement other than BM.

Abbreviations: FL, follicular lymphoma; HR, hazard ratio; CI, confidence interval; FLIPI, Follicular Lymphoma International Prognostic Index; ECOGPS, Eastern Cooperative Oncology Group Performance Status; BM, bone marrow; ALC, absolute lymphocyte count; HBsAg, hepatitis B surface antigen; HBeAg, hepatitis B e antigen; POD24, progression of disease within 24 months; R-CHOP, cyclophosphamide, doxorubicin, vincristine and prednosine plus rituximab; BR, bendamustine plus rituximab.

Table 5 Univariable Cox Regression Analysis with Respect to Progression-Free Survival and Overall Survival in HBsAg+ Subgroup

	PFS			OS		
	HR	**95% CI**	***P* value**	**HR**	**95% CI**	***P* value**
Age (≥60 vs <60)	1.484	0.815–2.702	0.194	3.713	1.496–9.213	**0.002**
Sex (male vs female)	1.178	0.644–2.152	0.595	0.906	0.384–2.137	0.822
Grade (3A va 1–2)	1.319	0.699–2.490	0.393	1.410	0.538–3.693	0.485
Ann Arbor stage (III/IV vs I/II)	1.212	0.579–2.538	0.609	1.085	0.395–2.983	0.874
Number of extranodal sites (<5 vs ≥5)[a]	0.899	0.493–1.639	0.727	0.883	0.370–2.108	0.779
B symptoms (yes vs no)	0.925	0.400–2.265	0.911	3.278	1.216–8.838	**0.013**
BM involvement (no vs yes)	0.514	0.159–1.663	0.258	0.041	0.000–23.589	0.126
High FLIPI risk	2.763	0.820–9.311	0.101	9.455	1.068–3.671	0.053
Elevated LDH level	1.616	0.840–3.109	0.147	3.891	1.645–9.202	**0.001**
Serum albumin <3.5 g/dL	1.893	0.737–4.860	0.177	4.217	1.352–3.156	**0.007**
ALC <1000 /μL	3.275	0.998–10.748	**0.038**	2.598	1.001–5.485	0.344
HBeAg positivity	1.218	0.538–2.757	0.635	1.062	0.311–3.642	0.923
High HBV-DNA load (>10^5 copies/mL)	3.103	1.638–5.878	**<0.001**	2.184	0.893–5.342	0.079
Viral load decline within 1 month (no vs yes)	1.051	0.577–1.915	**0.027**	0.580	0.233–1.446	0.237
Treatment (BR vs R-CHOP)	2.014	0.744–5.451	**0.048**	1.143	0.467–2.796	0.770

Notes: *All potential prognostic factors for progression-free survival with a P value less than 0.1 in the univariate analysis were selected for multivariate analysis using the backward elimination method (Wald test). [a]Extranodal sites of involvement other than BM. *P* value <0.05 was showed in bold.
Abbreviations: FL, follicular lymphoma; HR, hazard ratio; CI, confidence interval; FLIPI, Follicular Lymphoma International Prognostic Index; ECOGPS, Eastern Cooperative Oncology Group Performance Status; BM, bone marrow; ALC, absolute lymphocyte count; HBsAg, hepatitis B surface antigen; HBeAg, hepatitis B e antigen; R-CHOP, cyclophosphamide, doxorubicin, vincristine and prednosine plus rituximab; BR, bendamustine plus rituximab.

Methylation Profiling Distinguish in Sequential Pre-POD24-FL and POD24-FL with HBsAg+

As previous studies of susceptible methylation in FL had been limited to the initial stage of disease,[19] we investigated paired pre-POD24-HBsAg+ and POD24-HBsAg+ biopsies in FL to determine whether there was a dynamic alteration in methylation status over time with disease progression. Significant high methylation in 2029 Differentially Methylated Positions (DMPs) in POD24-HBsAg+ FL relative to pre-POD24 sample (*P* value < 0.01 and $\Delta\beta \geq 0.2$; Figure 3A–C) and showed predominantly discrepant profiles in POD24 stage (Figure 3D). 6.3% (40/632) Cytosine-Phosphate-Guanine (CpG) loci were aggregated near to the downstream 2.5 kb from transcription start sites (TSS) and 9.3% (59/632) were near to the upstream 2.5kb sites in pre-POD24-HBsAg+ FL, but almost none located in TSS. Notably, 6.2% (39/632) CpG loci were located within the TSS in POD24-HBsAg+ FL ($P \leq 0.01$, Figure 3E and F).

Correlation with Gene Expression of Tumor Immunity

Presented based on algorithm of methylation signatures, we found a higher infiltration of CD4+ T-cells ($P = 0.013$), monocytes ($P = 0.008$), and natural killer cells ($P = 0.004$), but lower proportions of nonmalignant B cells (P = 0.005) and a lower lymphocyte-to-monocyte ratio (0.85 vs 6.03) in POD24-HBsAg+ than in pre-POD24-HBsAg+ sample. No significant changes of intratumoral CD8+ T cells ($P = 0.341$) and neutrophils ($P = 0.175$) between two groups (Supplementary Figure 3 and Supplementary Table 3). 682 DMPs corresponding to immune function-related genes (eg IL32, ITK, NCR2, MHC I class molecular) were identified in POD24-HBsAg+ compared to pre-POD24-HBsAg+ (Figure 3G and Supplementary Table 4).

One hundred and ninety-six DMPs showed a significant correlation with gene expression involved in the tumor immunity process (Supplementary Figures 4 and 5). For example, CXCR5, TNFRSF10B, HLA-DQB1, RUNX1 and CTH were observed incremental methylation in POD24-HBsAg+ FL while ITGB2, TBX21 and NCF4 were over-represented in pre-POD24-HBsAg+ FL. KMT2A, EP300-AS1, and ARID1B related to malignant transformation effect[20] were methylated, while MYC related to aggressive transformation was defective methylation (Supplementary Table 4).

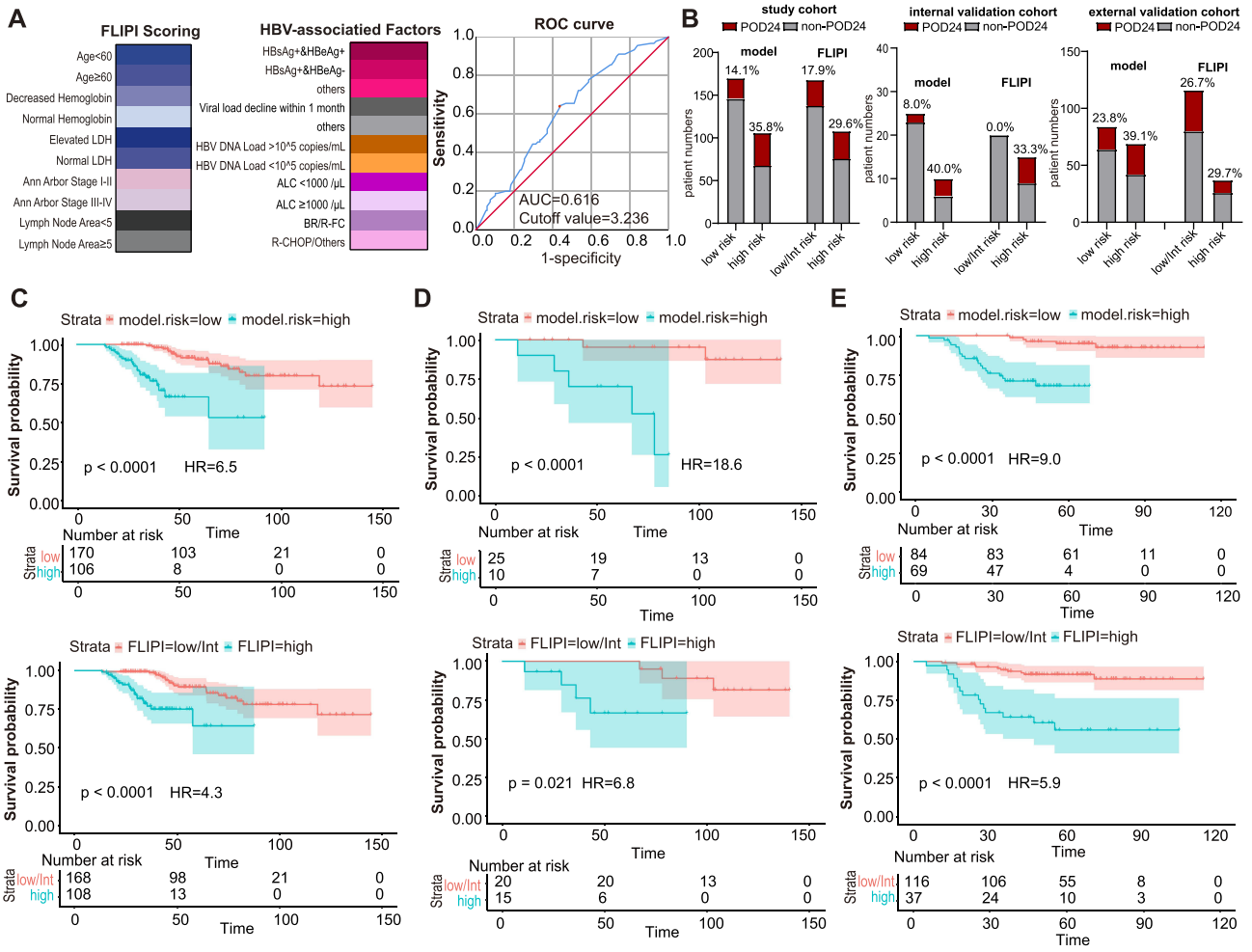

Figure 2 HBV-related risk factors slightly improved the risk stratification based on FLIPI scoring. (**A**) The constitutions of risk stratification are showed by colorful graphs with canonical FLIPI and five HBV-associated parameters. Each classification uses a set of decreasing colors. The best cutoff value of 3.236 for the new risk stratification with AUC of 0.616 were evaluated by ROC curve. (**B**) The proportion of POD24 events in risk stratification of model and FLIPI, in study cohort, in internal validation cohort, and in external validation cohort, respectively. Risk groups for overall survival (OS, month) were assessed by Kaplan–Meier survival curves based on the new risk stratifications (upper) and FLIPI scoring (below) in study cohort (**C**), in internal validation cohort (**D**), and in external validation cohort (**E**).
Abbreviations: AUC, Area under Curve; ROC, Receiver Operating Characteristic.

Our CpG datasets were extensively overlapped in immune-regulated genes profiling[21] noted in GSE14582.[22] Seed cluster analysis showed the interaction network center on TNFRSF1A (GSE23002), ACTG1, IQCE and LTA (GSE131559) in POD24-HBsAg+ FL. The FOXP1, MLH3, UBQLN1, and MTA1 were significantly over-represented in pre-POD24-HBsAg+ FL (Figure 4 and Supplementary Tables 4, 5).

High-density DNA methylation arrays allow for determining copy number alterations, and frequently encountered alteration include segmental chromosomal amplifications of ITK, IL7R, CD14, and TNFAIP8 in POD24-HBsAg+ FL. Whereas, segmental chromosomal deletions of IL21R, TGFB1I1, and TNFRSF12A were also related to POD24 occurrence (Supplementary Figure 6 and Supplementary Tables 6, 7).

Validation of the Correlation Between CpG Methylation and mRNA Expression

We performed whole transcriptome sequencing (RNA-seq) of 6 biopsies samples from another patient cohorts with HBsAg+ FL (n = 3, pre- and POD24-matched samples). We searched for associations between DEGs expressions (log2FC) and mCpG dela beta values located 200kb upstream of TSS. In POD24-HBsAg+ FL, out of 2877 low-methylated ($\Delta\beta \leq -0.2$) sequences, 454 DEGs were upregulated involved in metabolism-enhanced genes (SLC2A2,[23] GLS2[24]) and immunosuppressive molecules (IL1R2, IL22RA1[25]). Notably, 969 promoter methylations contained 115

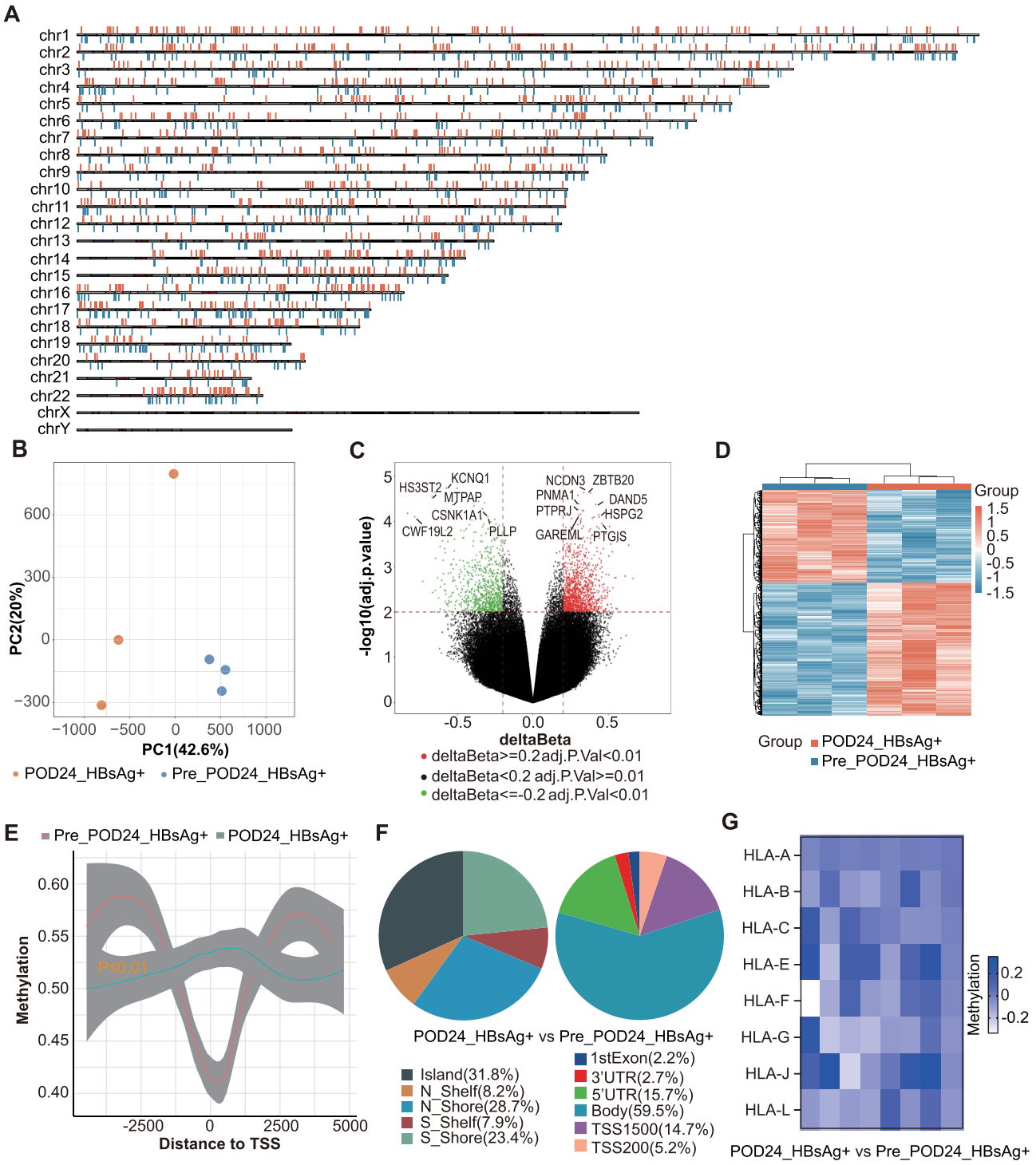

Figure 3 Multiple differential methylation positions (DMPs) with distinct distributions among pre-POD24-HBsAg+FL and paired POD24-HBsAg+FL. (**A**) The schematic map shows the distribution of DMPs on each chromosome succinctly. Hypermethylated and hypomethylated CpGs are represented in Orange and blue respectively. (**B**) The scatter plots show the differences of CpGs between groups. The orange points represent DMPs, and the blue points represent undifferentiated points. (**C**) The volcano plots show the Δβ and significance of CpGs between groups. The upper right region and the upper left region represent hypermethylated and hypomethylated points with statistical differences respectively. (**D**) Heat maps were used to view the similarity of samples between groups after z-Score scaling. (**E**) The methylation differences of 5kb upstream and downstream of TSS between groups. (**F**) The pie chart shows the distribution of CpG islands (left) and gene regions (right). (**G**) The Heatmap showed the different methylation of MHC class I genes.

https://doi.org/10.2147/ITT.S543117

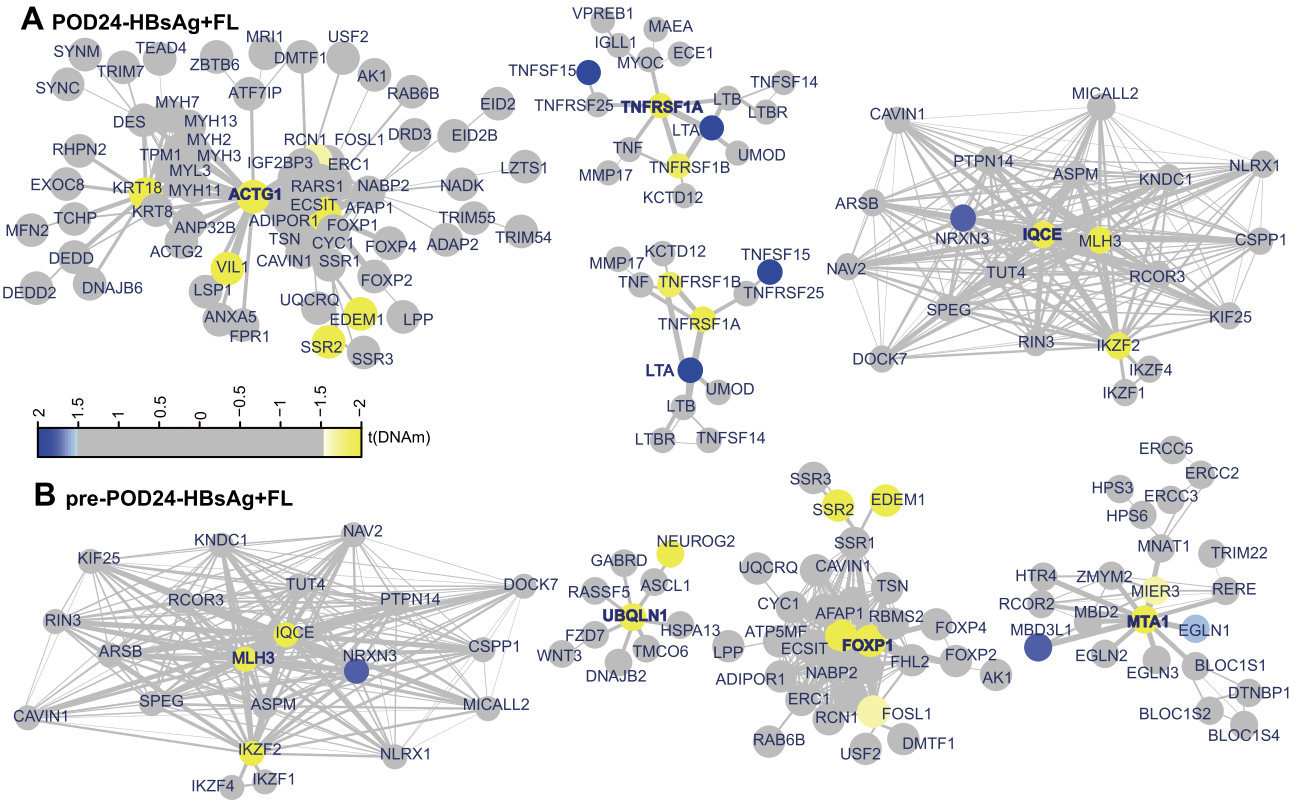

Figure 4 Functional Epigenetic Modules showed seed gene (**A**) TNFRSF1A-, ACTG1-, IQCE-, LTA-interaction network in POD24-HBsAg+FL tumors and (**B**) FOXP1-, MLH3-, UBQLN1- and MTA1-interaction network in pre-POD24-HBsAg+FL. Each node is a gene, and the color of the node presents statistical significance of their contribution to the disease regulation. Blue for positive significance, yellow for negative significance, and gray for no difference. The line between nodes is the degree of connectivity between genes, and the thickness of the line represents the level of correlation.

associated down-regulated mRNA expression matched to the abovementioned (ITGB2, IL21R, C1QB[26]) (Figure 5A). Generally, the gene with up-regulated expression primarily existed in low-methylation status (quantile) at TSS200 in POD24-HBsAg+ FL compared to pre-POD24-HBsAg+ FL (Figure 5B). Top DEGs expression (FPKM values) correlated to distinct promoter methylation sites within top specific chromosome regions (60%), also known as imprinted regions, which were expected as modifiers for expression of origin (Figure 5C and D). We next captured the methylation sites highly correlated to the CXCR5 mRNA expression were simultaneously less correlated to the mRNA expression of MYC gene (Figure 5E). These two genes were also known as mover for malignant progression of B cell,[27,28] which was representative acting as the "trans" correlations existing universally between different genes. Interestingly, "cis" correlations between same gene were showed that methylation sites were simultaneously highly or low correlated with in mRNA expression, especially existing in CXCR5 (body, spearman 0.94; top 1) which was calculated around three methylation sites on average presenting strong correlation with enhanced mRNA expression in POD24-HBsAg+ FL (Figure 5F).

The Impact of CXCR5 on Aggressive MYC-B Cells

Given about 10% to 15% of patients with aggressive B-cell lymphoma have MYC gene rearrangement, we confirmed that MYC mRNA expression was strongly correlated to low-methylation level in POD24-HBsAg+ FL compared with pre- POD24-HBsAg+ FL (TSS200, Pearson 0.059, $P < 0.0001$; Figure 5A). We further considered aggressive immunogenic model from Myc-Cd19-Cre mice to infer the B-cell progressive mechanism by other methylated genes at transcriptional activation in MYC variants context. Compared with wild type C57BL/6J mice histologically, $MYC^{+/+}$ CD19-B cell lymphoma presented lymphoma cells, with medium size, with giant cells and atypia, irregular nuclei and presence of mitotic sign (Figure 6A). Furthermore, RNA-seq from $MYC^{+/+}$ CD19-B cell lymph node displayed increased

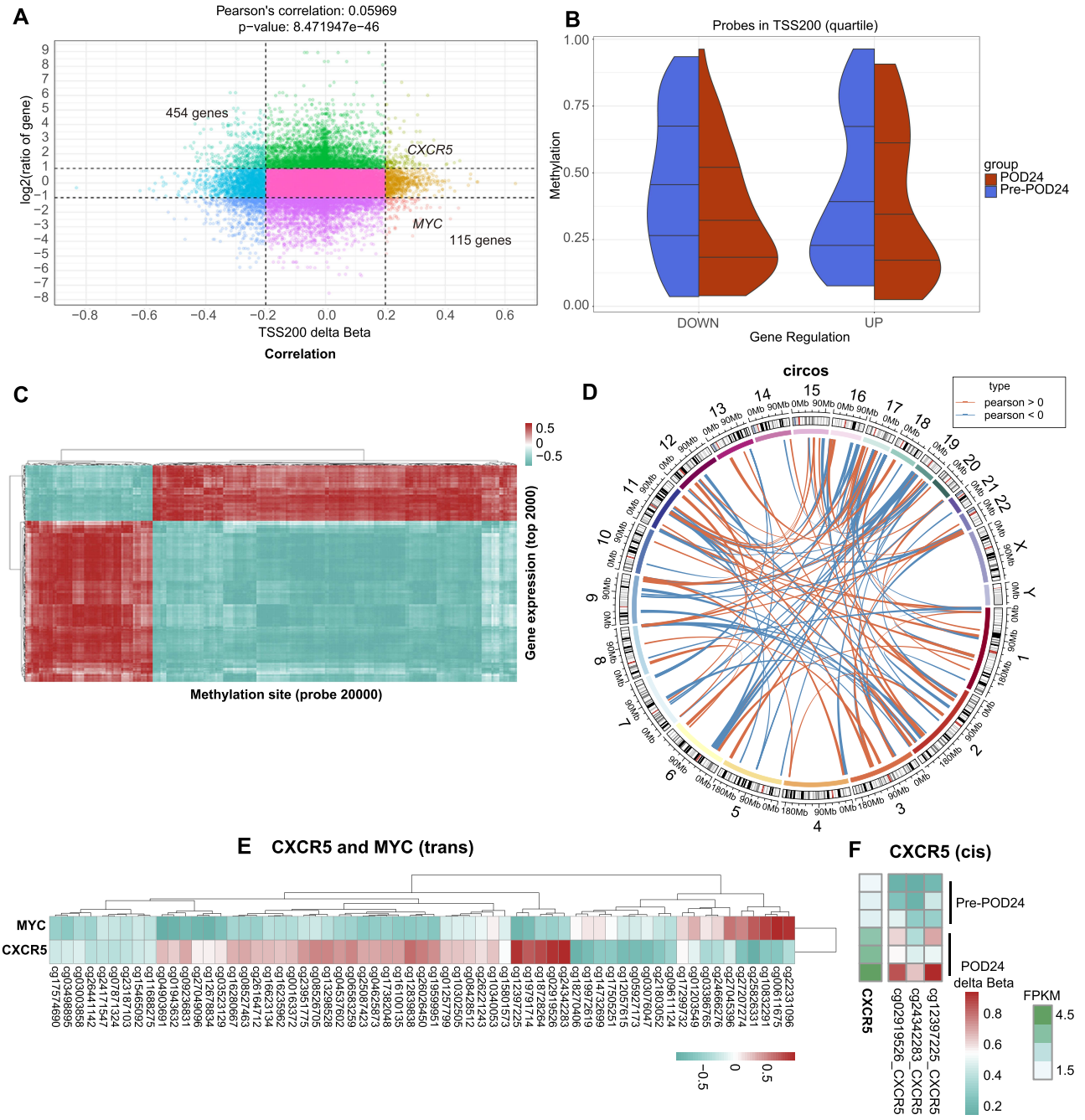

Figure 5 Correlation of methylation sites and gene expression. (**A**) Scatterplot corresponds to the associations found between methylation (delt beta at TSS200, x axis) and gene expression (logFC, y axis). (**B**) The splitviolins plots depicting the distribution of CpG site methylations in DEGs from two samples. Quantile 25%, 50%, 75% lines are shown. The distributions from pre-POD24-HBsAg+FL and paired POD24-HBsAg+FL samples are colored in red and blue respectively. The heatmap (**C**) and the Circos plot (**D**) depicting the distribution of associations between CpG site methylation and the level of expression of the corresponding genes. Spearman correlation is used as measure. Euclidean distance and complete method are used in bi-clustering. The outer circle represents different chromosome numbers, and the inner circle may be refined to specific positions in the genome. The correlation was showed by connecting lines. (**E**) The heatmap specifically depicting the distribution of associations between same CpG site methylation and the level of expression of the distant genes involving in CXCR5 and MYC. (**F**) Spearman correlation coefficient including Beta value of relevant methylation site location information and FPKM value of CXCR5 gene expression in a specific gene region.

CXCR5 mRNA level in line with the global changes from $MYC^{+/+}$ malignant B cells compared to $MYC^{-/-}$ mice. The chemokine activity of the receptor itself did appear to be aberrantly activated in $MYC^{+/+}$ malignant B cells (Figure 6B). Although observed distinct transcriptional enhance of CXCR5 among POD24-HBsAg+ FL ($P = 0.00064$) involved in silencing chemokine receptors binding, interferon and immunoregulatory interaction between lymphoid cells signaling,

https://doi.org/10.2147/ITT.S543117

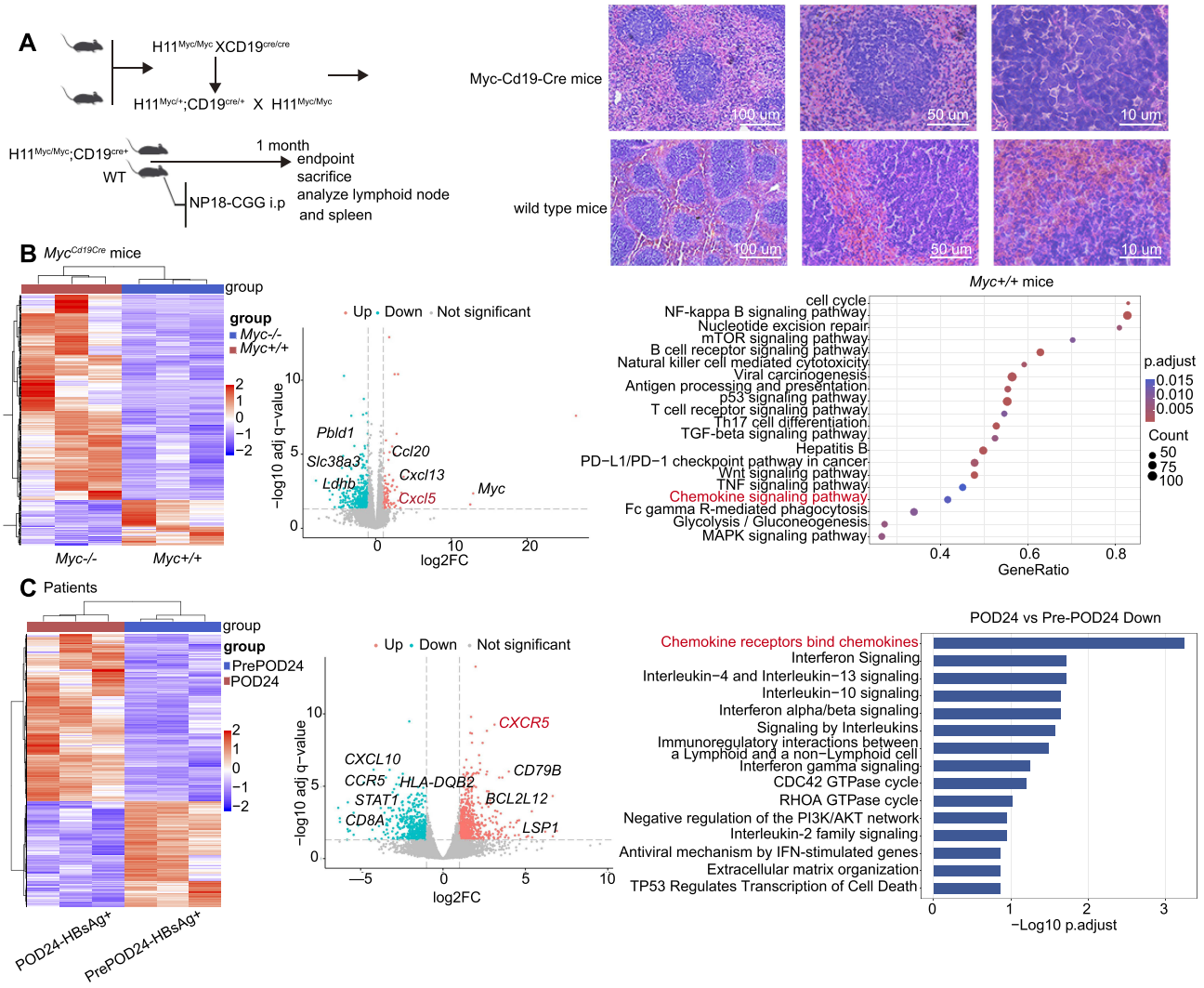

Figure 6 The impact of CXCR5 expression on aggressive MYC-B cells development. (**A**) Experimental scheme of mice model and timeline. H&E of spleen sections from mice. Scale, 100 μm (left) 50 μm (center) or 10 μm (right). (**B**) RNA-seq with DEGs profiling in chimera mice, involving in Heatmap, volcano and KEGG enrichment graphic. (**C**) RNA-seq of DEGs profile between pre-POD24-HBsAg+FL and paired POD24-HBsAg+FL samples, presented with Heatmap, volcano and KEGG enrichment graphic. Red highlighted CXCR5 gene and related critical pathway.

there was defective in MYC transcription with functional categories (Figure 6C). This finding suggests that the CXCR5 pathways depicted in Figure 6B is driven by the overall transcription shift of MYC in malignant B cells towards a more paused, less proliferative state which the MYC-pathway is often associated (eg p53, mTOR signaling pathway).

Discussion

FL is known to be a disease of immune dysfunction and is susceptible to infectious pathogens, mainly viruses.[29] Risk-adapted treatment approaches including immunochemotherapy (eg R-CHOP, BR) and inevitable prophylactic NAT should be prioritized at the high-risk FL populations. Although anti-HBV therapy was strongly recommended in HBsAg+ patients regardless of HBV DNA levels,[30] HBV infection associated with inferior survival[5] is not really on the risk list. The risk evaluation results were not upgraded by patients with heavy HBV infection and we may misjudge a high-risk patient. We consequently designed this study to investigate that not only HBsAg-positive factor but also HBV-induced immune activities should be dependent prognostic indicators. Three aspects are important to be cautious about POD24 event that firstly, accompanying time with HBV infection,[31] which may be ascribed to the persistent antigen stimulation for exhausted immune states.[32] Second, the active status of HBV replication, which could be

interpreted by that a small fraction of antigen-specific CD8+ T cells survived and formed long-lasting memory T cells in an acute inflammatory context, which remained the effective functions upon encountering antigens.[33] Third, the immunosuppressive effect from cytotoxic chemotherapy with decreased ALC, which may owe to the B cell lymphopenia caused by drugs like bendamustine[34] and indirectly affect the T-cell infiltrations due to the loss of B-cell helper especially within intra-tumoral tertiary lymphatic structure.[33]

Indeed, our result assigned a novel risk stratification that integrates HBV-related[16] and immune-regulated[35] clinical factors into FLIPI system, could contribute to enhancing identification of high-risk patients than FLIPI scoring alone, and importantly, validated by a series of patients cohorts from domestic multi-center clinical institution.

While clinically promising and practical in the abovementioned indicators, multiple studies demonstrated that a complex pattern of frequent mutations in epigenetic modifiers that are co-founding events arising during FL development and progression.[36] While epigenetic therapies such as histone deacetylase inhibitors (HDACi) have previously been evaluated in FL, the results were overall disappointing and pushed our further knowledge of the epigenomic landscape of this malignancy. DNA methylation with a significant overlap between hypermethylated CpGs and target genes in FL cells, especially the relapsed with POD24 or more aggressive tumors, followed by chemoimmunotherapy.[37] The initial conservation of methylation profiles was introduced with more measurable difference between paired pre- and post-POD24 HBsAg+ FL samples. The restricted number of genes with modifiable functional noncoding elements, including promoter and enhancers located proximal or distal to protein-coding genes, respectively, have for the most part been captured, including IL32, ITK, NCR2 and most methylated MHC class I genes,[38] which contributed to immunoinactivation and failed to response to immunotherapy.[39] Notably, we matched methylation site and correlated gene expression as RNA-seq and ranked the candidates by their correlation. We reasoned that CXCR5, which was dependent lymphoma cell dissemination and tumor-stroma interaction,[27] had strong methylation regions. Additionally, CXCR5 mRNA expression can be anti-correlated with the expression of MYC mRNA at the same methylation sites which acts as proto-oncogene[28] as "trans" candidate. We therefore posit that the biological connection of enhanced CXCR5 expression and MYC expression with developmental pausing may exist timely, as validated in $MYC^{+/+}$ ES cells of FL models. The roles in developmental contexts in which large-scale shifts in the transcriptional programme in these two crucial genes have to rapidly occur, which may constitute a more robust mechanism of POD24 process and new methyltransferase inhibitors to be recapitulated.

However, several challenges still remain to be addressed before they could be acted as critical markers: validation using molecular trials and extension in a larger cohort. The individual molecular predictor should be adjusted to be universally applicable. Some large and collaborative efforts are strived to address these problems. Interestingly, another study showed that anti-CXCR5 chimeric antigen receptor (CAR)-T cells eradicate B-NHL cells and lymphoma-supportive T follicular help cells,[27] showing the promising therapeutic values of CXCR5 target aligned with our findings.

We anticipate that the regulatory relationship between methylation and cellular dormancy will have implication that extend beyond identification. The insight here provides exciting new opportunities to developmental therapies of interest to diapause post-translational modifications, strongly wishing to delay POD24 transition in the context of HBV interference.

Conclusions

Integrated HBV-related clinicopathological features into FLIPI scoring system may provide precise pre-treatment risk stratification for HBV-positive FL. Modifiable DNA methylation acts as the potential targets for the combined treatment strategy to delay POD24 occurrence in high-risk HBV-positive FL.

Abbreviations

FL, follicular lymphoma; FLIPI, Follicular Lymphoma International Prognostic Index; HBV, Hepatitis B virus; HBsAg, Hepatitis B surface antigen; OS, overall survival; POD24, progression of disease within 24 months; NAT, nucleoside analogues treatment; PFS, progression-free survival; AUC, Area Under Curve; ROC, Receiver Operating Characteristic; CXCR5, Chemokine C-X-C-Motif Receptor 5; MYC, Myelocytomatosis oncogene; TSS, transcription start sites; DMPs, Differentially Methylated Positions.

Data Sharing Statement

Bulk RNA-seq raw datasets were published in Zenodo with DOI: https://zenodo.org/records/15308886 for six human samples and https://zenodo.org/records/15308591 for six Chimeric mice. Illumina Methylation EPIC BeadChip raw data were published in Zenodo with DOI: https://zenodo.org/records/15354057 in human FFPE samples. Data are now restricted and will be also available on Zenodo as of the date of publication. Other data generated during the current study are available from the corresponding author Prof. Jianli Ma.

Ethics Approval and Consent to Participate

For human samples, all study procedures were approved by the Institutional Review Boards (IRBs) of the Harbin Medical University Cancer (Approval no. EC-20210408-1011 and no. KY2023-79). All participating patients provided written informed consent. This study was performed in accordance with the Declaration of Helsinki. The experimental procedures were performed in strict accordance with the institutional guidelines delineated by Harbin Medical University, the Guide for the Care and Use of Laboratory Animals, and standards established by the Association for Assessment and Accreditation of Laboratory Animal Care International. The Southern Model Biology Research Center (Shanghai), the Institutional Animal Care and Use Committee of Harbin Medical University, and Harbin Veterinary Research Institute, Chinese Academy of Agricultural Sciences, vetted all procedures and duly approved the entirety of the study involving mice under protocols # HMUIRB2025004, and #SCXK(shanghai)2019-0002.

Patient Consent for Publication

Acquired.

Acknowledgments

We appreciate all the patients participated. Sinotech Genomics Co., Ltd provides the technique support. The clinical data collection and partial sample provision are supported by the Harbin Medical University Cancer Hospital, the Tianjin Medical University Cancer Institute and Hospital, the Fourth Hospital of Hebei Medical University, the Shandong University Cancer Center, the First Affiliated Hospital of Harbin Medical University, and the Henan Cancer Hospital. The authors would like to thank all the reviewers who participated in the review, as well as MJEditor (www.mjeditor.com) for providing English editing services during the preparation of this manuscript.

Author Contributions

All authors made a significant contribution to the work reported, whether that is in the conception, study design, execution, acquisition of data, analysis and interpretation, or in all these areas; took part in drafting, revising or critically reviewing the article; gave final approval of the version to be published; have agreed on the journal to which the article has been submitted; and agree to be accountable for all aspects of the work.

Funding

Supporting funds from the Youth Project of National Natural Science Foundation of China (No.82303299), Haiyan Foundation Distinguished Young Scholar Program (No. JJJQ2024-03), Haiyan Foundation Outstanding Young Scholar Program (No. JJYQ2024-01), Key Research and Development Program Project of Heilongjiang Province (No. 2023ZX06C08) and the New Era Longjiang Excellent Doctoral Dissertation Project (No. LJYXL2022-65).

Disclosure

The authors reported no competing interests in this work.

References

1. Carbone A, Roulland S, Gloghini A, et al. Follicular lymphoma. *Nat Rev Dis Primers*. 2019;5(1):83.
2. Guo S, Chan JK, Iqbal J, et al. EZH2 mutations in follicular lymphoma from different ethnic groups and associated gene expression alterations. *Clin Cancer Res*. 2014;20(12):3078–3086. doi:10.1158/1078-0432.CCR-13-1597

3. Ardeshna KM, Qian W, Smith P, et al. Rituximab versus a watch-and-wait approach in patients with advanced-stage, asymptomatic, non-bulky follicular lymphoma: an open-label randomised Phase 3 trial. *Lancet Oncol*. 2014;15(4):424–435. doi:10.1016/S1470-2045(14)70027-0
4. Freedman A, Jacobsen E. Follicular lymphoma: 2020 update on diagnosis and management. *Am J Hematol*. 2020;95(3):316–327. doi:10.1002/ajh.25696
5. Cheng CL, Fang WQ, Lin YJ, et al. Hepatitis B surface antigen positivity is associated with progression of disease within 24 months in follicular lymphoma. *J Cancer Res Clin Oncol*. 2022;148(5):1211–1222. doi:10.1007/s00432-021-03719-y
6. Zhao X, Guo X, Xing L, et al. HBV infection potentiates resistance to S-phase arrest-inducing chemotherapeutics by inhibiting CHK2 pathway in diffuse large B-cell lymphoma. *Cell Death Dis*. 2018;9(2):61. doi:10.1038/s41419-017-0097-1
7. Jeong SH. Treatment of indolent lymphoma. *Blood Res*. 2022;57(S1):120–129. doi:10.5045/br.2022.2022054
8. Cao X, Wang Y, Li P, Huang W, Lu X, Lu H. HBV reactivation during the treatment of non-hodgkin lymphoma and management strategies. *Front Oncol*. 2021;11:685706. doi:10.3389/fonc.2021.685706
9. Batlevi CL, Sha F, Alperovich A, et al. Follicular lymphoma in the modern era: survival, treatment outcomes, and identification of high-risk subgroups. *Blood Cancer J*. 2020;10(7):74. doi:10.1038/s41408-020-00340-z
10. Alig S, Jurinovic V, Pastore A, et al. Impact of age on clinical risk scores in follicular lymphoma. *Blood Adv*. 2019;3(7):1033–1038. doi:10.1182/bloodadvances.2019032136
11. Lu Y, Yu J, Gong W, et al. An Immune-Clinical Prognostic Index (ICPI) for patients with de novo follicular lymphoma treated with R-CHOP/CHOP chemotherapy. *Front Oncol*. 2021;11:708784. doi:10.3389/fonc.2021.708784
12. Ren W, Wang X, Yang M, et al. Distinct clinical and genetic features of hepatitis B virus-associated follicular lymphoma in Chinese patients. *Blood Adv*. 2022;6(9):2731–2744. doi:10.1182/bloodadvances.2021006410
13. Shen J, Dai J, Zhang Y, et al. Baseline HBV-DNA load plus AST/ALT ratio predicts prognosis of HBV-related hepatocellular carcinoma after hepatectomy: a multicentre study. *J Viral Hepat*. 2021;28(11):1587–1596. doi:10.1111/jvh.13606
14. Isshiki Y, Chen X, Teater M, et al. EZH2 inhibition enhances T cell immunotherapies by inducing lymphoma immunogenicity and improving T cell function. *Cancer Cell*. 2025;43(1):49–68.e49. doi:10.1016/j.ccell.2024.11.006
15. Araujo-Ayala F, Béguelin W. Biology as vulnerability in follicular lymphoma: genetics, epigenetics, and immunogenetics. *Blood*. 2025;146:1759–1769. doi:10.1182/blood.2024026020
16. Lemaitre M, Brice P, Frigeni M, et al. Hepatitis B virus-associated B-cell non-Hodgkin lymphoma in non-endemic areas in Western Europe: clinical characteristics and prognosis. *J Infect*. 2020;80(2):219–224. doi:10.1016/j.jinf.2019.12.005
17. Lau GK, Leung YH, Fong DY, et al. High hepatitis B virus (HBV) DNA viral load as the most important risk factor for HBV reactivation in patients positive for HBV surface antigen undergoing autologous hematopoietic cell transplantation. *Blood*. 2002;99(7):2324–2330. doi:10.1182/blood.V99.7.2324
18. Zheng SC, Breeze CE, Beck S, Teschendorff AE. Identification of differentially methylated cell types in epigenome-wide association studies. *Nat Methods*. 2018;15(12):1059–1066. doi:10.1038/s41592-018-0213-x
19. Korfi K, Ali S, Heward JA, Fitzgibbon J. Follicular lymphoma, a B cell malignancy addicted to epigenetic mutations. *Epigenetics*. 2017;12(5):370–377. doi:10.1080/15592294.2017.1282587
20. Araf S, Okosun J, Koniali L, Fitzgibbon J, Heward J. Epigenetic dysregulation in follicular lymphoma. *Epigenomics*. 2016;8(1):77–84. doi:10.2217/epi.15.96
21. Dave SS, Wright G, Tan B, et al. Prediction of survival in follicular lymphoma based on molecular features of tumor-infiltrating immune cells. *N Engl J Med*. 2004;351(21):2159–2169. doi:10.1056/NEJMoa041869
22. O'Riain C, O'Shea DM, Yang Y, et al. Array-based DNA methylation profiling in follicular lymphoma. *Leukemia*. 2009;23(10):1858–1866. doi:10.1038/leu.2009.114
23. Deng M, Liao S, Deng J, et al. S100A2 promotes clear cell renal cell carcinoma tumor metastasis through regulating GLUT2 expression. *Cell Death Dis*. 2025;16(1):135. doi:10.1038/s41419-025-07418-1
24. Feng S, Aplin C, Nguyen TT, Milano SK, Cerione RA. Filament formation drives catalysis by glutaminase enzymes important in cancer progression. *Nat Commun*. 2024;15(1):1971. doi:10.1038/s41467-024-46351-3
25. Guo H, Liu C, Wu K, Li Y, Zhang Z, Chen F. Single-cell RNA sequencing reveals an IL1R2+Treg subset driving immunosuppressive microenvironment in HNSCC. *Cancer Immunol Immunother*. 2025;74(5):159. doi:10.1007/s00262-025-04015-1
26. Thomas MF, Slowikowski K, Manakongtreecheep K, et al. Single-cell transcriptomic analyses reveal distinct immune cell contributions to epithelial barrier dysfunction in checkpoint inhibitor colitis. *Nat med*. 2024;30(5):1349–1362. doi:10.1038/s41591-024-02895-x
27. Bunse M, Pfeilschifter J, Bluhm J, et al. CXCR5 CAR-T cells simultaneously target B cell non-Hodgkin's lymphoma and tumor-supportive follicular T helper cells. *Nat Commun*. 2021;12(1):240. doi:10.1038/s41467-020-20488-3
28. Hilton LK, Collinge B, Ben-Neriah S, et al. Motive and opportunity: MYC rearrangements in high-grade B-cell lymphoma with MYC and BCL2 rearrangements (an LLMPP study). *Blood*. 2024;144(5):525–540. doi:10.1182/blood.2024024251
29. Jelicic J, Stauffer Larsen T, Bukumiric Z, Andjelic B. The clinical applicability of current prognostic models in follicular lymphoma: a systematic review. *Crit Rev Oncol Hematol*. 2021;164:103418. doi:10.1016/j.critrevonc.2021.103418
30. Pastore A, Jurinovic V, Kridel R, et al. Integration of gene mutations in risk prognostication for patients receiving first-line immunochemotherapy for follicular lymphoma: a retrospective analysis of a prospective clinical trial and validation in a population-based registry. *Lancet Oncol*. 2015;16(9):1111–1122. doi:10.1016/S1470-2045(15)00169-2
31. Yuen MF, Chen DS, Dusheiko GM, et al. Hepatitis B virus infection. *Nat Rev Dis Primers*. 2018;4:18035. doi:10.1038/nrdp.2018.35
32. Liu X, Li M, Wang X, et al. PD-1(+) TIGIT(+) CD8(+) T cells are associated with pathogenesis and progression of patients with hepatitis B virus-related hepatocellular carcinoma. *Cancer Immunol Immunother*. 2019;68(12):2041–2054. doi:10.1007/s00262-019-02426-5
33. Philip M, Schietinger A. CD8(+) T cell differentiation and dysfunction in cancer. *Nat Rev Immunol*. 2022;22(4):209–223. doi:10.1038/s41577-021-00574-3
34. Gafter-Gvili A, Polliack A. Bendamustine associated immune suppression and infections during therapy of hematological malignancies. *Leuk Lymphoma*. 2016;57(3):512–519. doi:10.3109/10428194.2015.1110748
35. Zhou X, Pan H, Yang P, Ye P, Cao H, Zhou H. Both chronic HBV infection and naturally acquired HBV immunity confer increased risks of B-cell non-Hodgkin lymphoma. *BMC Cancer*. 2019;19(1):477. doi:10.1186/s12885-019-5718-x

36. Hayslip J, Montero A. Tumor suppressor gene methylation in follicular lymphoma: a comprehensive review. *Mol Cancer*. 2006;5:44. doi:10.1186/1476-4598-5-44
37. Lu L, Yoshimoto K, Morita A, Kameda H, Takeuchi T. Bendamustine increases interleukin-10 secretion from B cells via p38 MAP kinase activation. *Int Immunopharmacol*. 2016;39:273–279. doi:10.1016/j.intimp.2016.07.033
38. Luo N, Nixon MJ, Gonzalez-Ericsson PI, et al. DNA methyltransferase inhibition upregulates MHC-I to potentiate cytotoxic T lymphocyte responses in breast cancer. *Nat Commun*. 2018;9(1):248. doi:10.1038/s41467-017-02630-w
39. Gu SS, Zhang W, Wang X, et al. Therapeutically increasing MHC-I expression potentiates immune checkpoint blockade. *Cancer Discov*. 2021;11(6):1524–1541. doi:10.1158/2159-8290.CD-20-0812